AGU PUBLICATIONS

Earth and Space Science

RESEARCH ARTICLE
10.1002/2017EA000319

**Key Points:**
- CMIP5 models demonstrate similar variations of precipitation as observation, with positive (negative) trend over wet (dry) areas
- Positive (negative) trends of vertical velocity, cloud fractions, and condensed water path are found from models over wet (dry) areas
- The qualitatively consistent trends in these variables are important for a better understanding of the hydrological cycle

**Supporting Information:**
- Supporting Information S1

**Correspondence to:**
X. Jiang,
xjiang7@uh.edu

**Citation:**
Kao, A., X. Jiang, L. Li, H. Su, and Y. Yung (2017), Precipitation, circulation, and cloud variability over the past two decades, *Earth and Space Science*, *4*, 597–606, doi:10.1002/2017EA000319.

Received 5 JUL 2017
Accepted 22 AUG 2017
Accepted article online 24 AUG 2017
Published online 8 SEP 2017



# Precipitation, circulation, and cloud variability over the past two decades

**Angela Kao[1], Xun Jiang[1], Liming Li[2], Hui Su[3], and Yuk Yung[4]**

[1]Department of Earth and Atmospheric Sciences, University of Houston, Houston, Texas, USA, [2]Department of Physics, University of Houston, Houston, Texas, USA, [3]Science Division, Jet Propulsion Laboratory, California Institute of Technology, Pasadena, California, USA, [4]Division of Geological and Planetary Sciences, California Institute of Technology, Pasadena, California, USA

**Abstract** To better understand the variability of precipitation, circulation, and cloud, we examine the precipitation, vertical velocity, total cloud fraction, condensed water path, and ice water path from observations and 13 Coupled Model Intercomparison Project 5 (CMIP5) models over 1988–2008. All variables are averaged over wet areas and dry areas to investigate temporal variations of different variables over these regions. We found that all models demonstrate similar temporal variations of precipitation as the observational data from the Global Precipitation Climatology Project, with positive trend over wet areas (6.22 ± 3.75 mm/mon/decade) and negative trend over dry areas (−0.77 ± 0.54 mm/mon/decade). Positive trends of vertical velocity, total cloud fraction, condensed water path, and ice water path are also found in the observations and models over the wet areas. Observations also demonstrate decreasing trends of vertical velocity, total clouds, condensed water path, and ice water path over the dry areas, which can be simulated by most models with a few exceptions. The qualitatively consistent trends in these variables (i.e., vertical velocity, cloud, liquid, and ice water contents) as revealed from the observations and CMIPS models provide a clearer picture of the dynamics and physics behind the temporal variations of precipitation over different areas.

## 1. Introduction

Observational [*Adler et al*., 2003; *Gu et al*., 2007; *Adler et al*., 2008; *Li et al*., 2011] and modeling studies [*Allen and Ingram*, 2002; *Held and Soden*, 2006; *Stephens and Ellis*, 2008] suggest that the global precipitation exhibits only a weak positive trend over the past two decades, but regional precipitation may exhibit much stronger trends. In particular, previous studies [e.g., *Chou and Neelin*, 2004; *Allan and Soden*, 2007; *Chou et al*., 2009; *Li et al*., 2011; *Liu et al*., 2012; *Durack et al*., 2012; *Polson et al*., 2013; *Chou et al*., 2013; *Liu and Allan*, 2013; *Trammell et al*., 2015; *Donat et al*., 2016] suggest that the trend of precipitation is strongly positive over wet areas and strongly negative over dry areas. *Liu and Allan* [2013] have explored variation of precipitation over dry tropical land and noticed that simulation driven by the observed sea surface temperature can better simulate variability over land. *Greve et al*. [2014] found that dry (wet) gets drier (wetter) behavior is oversimplified over land. They noticed that ~11% of global land exhibits wet (dry) gets wetter (dryer), while ~9.5% global land area has the opposite pattern [*Greve et al*., 2014]. The regional precipitation variations are thought to relate to the increasing of greenhouse gases [*Allen and Ingram*, 2002; *Trammell et al*., 2015], temperature change [*Liu and Allan*, 2013; *Donat et al*., 2016], and the change of the difference between evaporation and precipitation [*Held and Soden*, 2006].

Different parameters, such as temperature, circulation, anthropogenic forcing, solar forcing, and clouds, can influence precipitation [*Trenberth and Shea*, 2005; *Shindell et al*., 2006; *Adler et al*., 2008; *Allan and Soden*, 2008; *Liu et al*., 2009; *Li et al*., 2011; *Bony et al*., 2013; *Su et al*., 2014; *Xie et al*., 2015; *Long et al*., 2016]. By analyzing the climate model outputs from the Coupled Model Intercomparison Project 5 (CMIP5), *Hegerl et al*. [2015] noticed that global precipitation increases when there is more greenhouse gas forcing. *Sun et al*. [2012] found that the largest changes in precipitation variance are over regions with the largest aerosol emissions. It is also found that the anthropogenic forcing can influence precipitation over different regions [*Zhang et al*., 2007; *Trammell et al*., 2015; *Wang et al*., 2015; *Sarojini et al*., 2016]. *Marvel and Bonfils* [2013] further suggested that increasing temperature and variations in the atmospheric circulation are related to the changes in precipitation. In addition to precipitation, cloud also demonstrates different trends at different regions [*Norris et al*., 2016]. A recent study by *Su et al*. [2017] found that most CMIP5 climate models underestimate the decrease

of tropical high cloud cover with increasing surface temperature and thus underestimate precipitation increase per unit surface warming.

In this paper, we investigate variations of precipitation, vertical velocity, cloud fraction, condensed water path, and ice water path over wet and dry areas to explore how well the models capture variations of different variables. These analyses can help us examine whether the models can successfully simulate these variations and characterize the variability of precipitation, circulation, and clouds at different regions. In addition, our analyses of these important variables related to the precipitation can help us better understand the dynamics and physics behind the temporal variations of precipitation over different regions.

## 2. Data and Models

The observational precipitation data used to compare and verify the accuracy of the models are from Global Precipitation Climatology Project (GPCP) [*Huffman et al*., 1997]. GPCP version 2.2 precipitation data are derived from different satellites and gauge measurements [*Huffman et al*., 2012]. The spatial resolution of GPCP version 2.2 precipitation is 2.5° × 2.5° (latitude by longitude). GPCP data are more reliable from 1988 to 2008, when it overlaps with Special Sensor Microwave Imager data [*Allan et al*., 2010]. Uncertainty of the GPCP precipitation product is estimated at ~15% [*Huffman et al*., 1997]. A total of 500 hPa vertical velocity data from National Centers for Environmental Prediction 2 (NCEP2) Reanalysis [*Kistler et al*., 2001] are also used to explore the circulation over wet and dry areas. The spatial resolution of NCEP2 vertical velocity is 2.5° × 2.5° (latitude by longitude). Total cloud fraction from the International Satellite Cloud Climatology Project (ISCCP) [*Norris et al*., 2016] is used to explore total cloud fraction over wet and dry areas. Variability related to satellite orbits and calibration is removed from ISCCP total cloud fraction [*Norris et al*., 2016]. The spatial resolution of ISCCP total cloud fraction is 2.5° × 2.5° (latitude by longitude). Condensed water path and ice water path from the European Center for Medium-Range Weather Forecasts (ECMWF) [*Delanoe et al*., 2011] will be used to explore liquid water and ice contents in clouds over wet and dry areas. The spatial resolution of ECMWF condensed water path and ice water path is 0.75° × 0.75° (latitude by longitude).

Precipitation, vertical velocity, cloud fractions, condensed water path, and ice water path from Atmosphere-Ocean Coupled Model Intercomparison Project 5 (CMIP5) [*Taylor et al*., 2012] model simulations are used in the paper. Observed sea surface temperature is used in the Atmospheric Model Intercomparison Project (AMIP)-type CMIP5 model simulations to drive the models [*Taylor et al*., 2012]. There are total 13 models used in this study, including Community Atmosphere Model 5 (CAM5), Canadian Centre for Climate Modelling and Analysis (CCCMA), Centre National de Recherches Météorologiques (CNRM), Commonwealth Scientific and Industrial Research Organisation (CSIRO), Geophysical Fluid Dynamics Laboratory (GFDL), Goddard Institute for Space Studies (GISS), Institute for Numerical Mathematics (INM), Institut Pierre-Simon Laplace (IPSL), Model for Interdisciplinary Research on Climate (MIROC), UK Met Office Hadley Climate Center (MOHC), Max-Planck-Institut (MPI), Meteorological Research Institute (MRI), and National Climate Centre (NCC). Validations of cloud and precipitation related fields in these models have been reported by many recent studies [e.g., *Dolinar et al*., 2014; *Jiang et al*., 2012; *Jiang et al*., 2015; *Stanfield et al*., 2016; *Su et al*., 2013; *Zhai et al*., 2015]. Since most of these models' AMIP-type simulations ended in 2008, we focus on the variations of different variables from both observation and model simulations from January 1988 to December 2008.

## 3. Methodology

To calculate variations of precipitation, vertical velocity, cloud, condensed water path, and ice water path over wet areas and dry areas, we first calculate the precipitation climatology over 1988–2008. Monthly mean precipiation is used in this paper. Precipitation amount in each month is estimated with a units of mm/mon. The wet and dry areas are defined as the areas with climatological monthly mean precipitation larger than 200 mm/mon and less than 50 mm/mon, respectively [see Figure 1 in *Trammell et al*., 2015]. A total of 200 mm/mon and 50 mm/mon are chosen as thresholds for wet and dry areas, so wet areas represent high precipitation areas over Intertropical Convergence Zone (ITCZ) and dry areas cover low precipitation areas in the subtropics and midlatitudes [*Trammell et al*., 2015; *Stanfield et al*., 2016]. Since the position of ITCZ changes as a function of months, we also conduct analyses to let wet and dry areas change positions following the ITCZ, which demonstrate similar results as the climatological wet and dry areas.

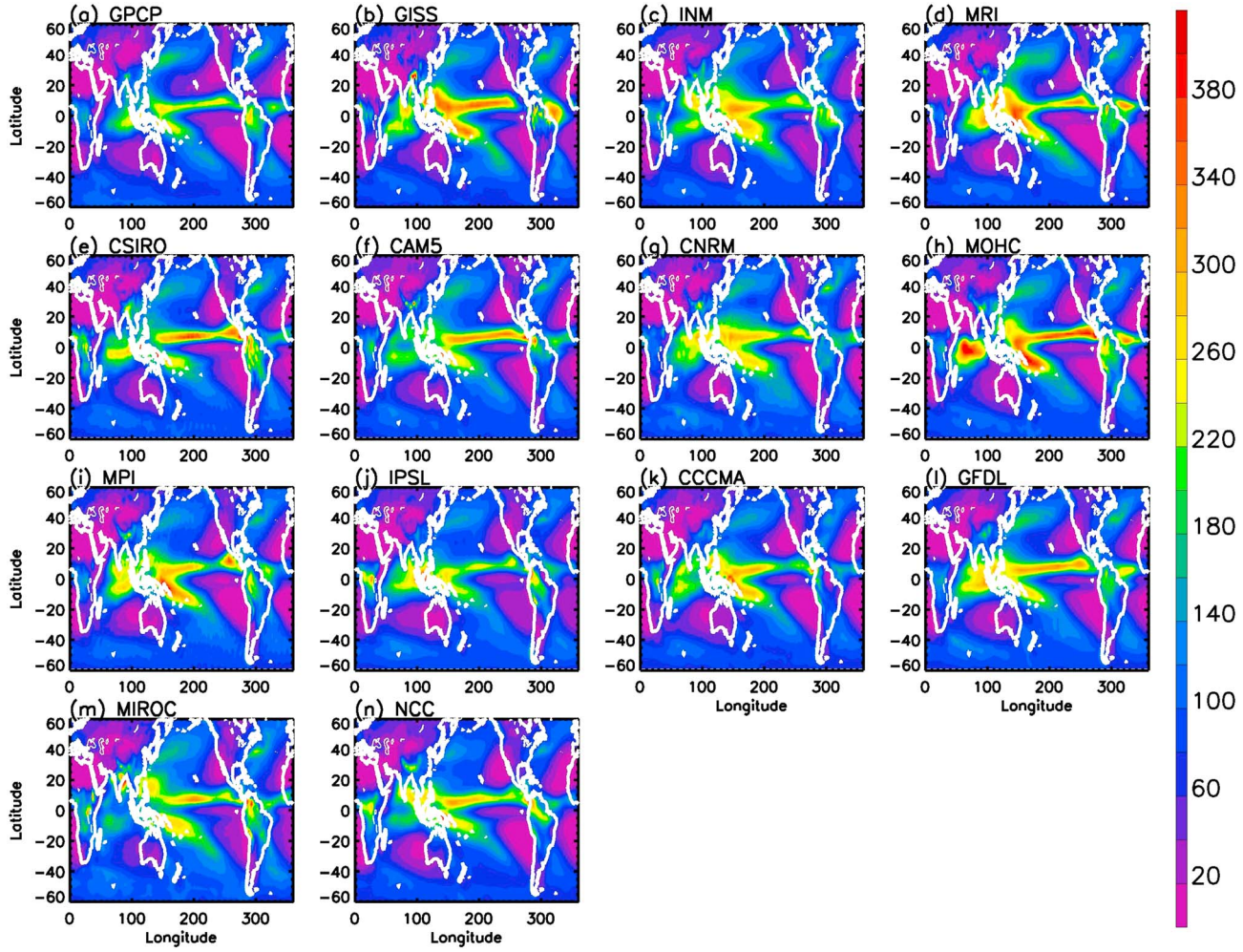


**Figure 1.** Spatial patterns of mean precipitation from GPCP and CMIP5 models for 1988–2008 over 60°S–60°N. Units are mm/mon.

A multiple regression method is applied to all time series to remove El Niño–Southern Oscillation (ENSO) signals from the time series [*Li et al*., 2011; *Trammell et al*., 2015]. First, the time series are regressed on Legendre polynomials, annual cycle, semiannual cycle, and Niño 3.4 index [*Li et al*., 2011]. The first, second, and third Legendre polynomials are used to represent the trend in the data sets. Niño 3.4 index is utilized to estimate ENSO signal in the time series. Then, the ENSO signal is subtracted from the time series. Finally, a low-pass filter is applied to all time series to remove signals with periods less than 3 years [*Jiang et al*., 2004].

## 4. Results

The spatial patterns of the observed climatological GPCP V2.2 precipitation and CMIP5 model precipitations for 1988–2008 are shown in Figure 1. As shown in Figure 1, high precipitation is overlapped with the ITCZ area, while low precipitation is over subtropical region. We apply 200 mm/mon and 50 mm/mon thresholds to individual model to identify wet and dry areas, so the wet/dry areas in different models are slightly different. Precipitation is averaged over the climatological wet areas ($P > 200$ mm/mon) and dry areas ($P < 50$ mm/mon) within 60°S–60°N. The results are shown in Figures 2a and 2c. GPCP precipitation is plotted as blue solid lines in Figures 2a and 2c. The anomaly around 1998 over both dry and wet regions is likely related to the Pacific decadal variability, as discussed by *Gu and Adler* [2013]. From the temporal variation of GPCP precipitation (blue solid lines), it is evident that the areas already receiving high precipitation tend to receive more with a trend of 9.09 ± 4.69 mm/mon/decade, while the areas already receiving little precipitation tend to

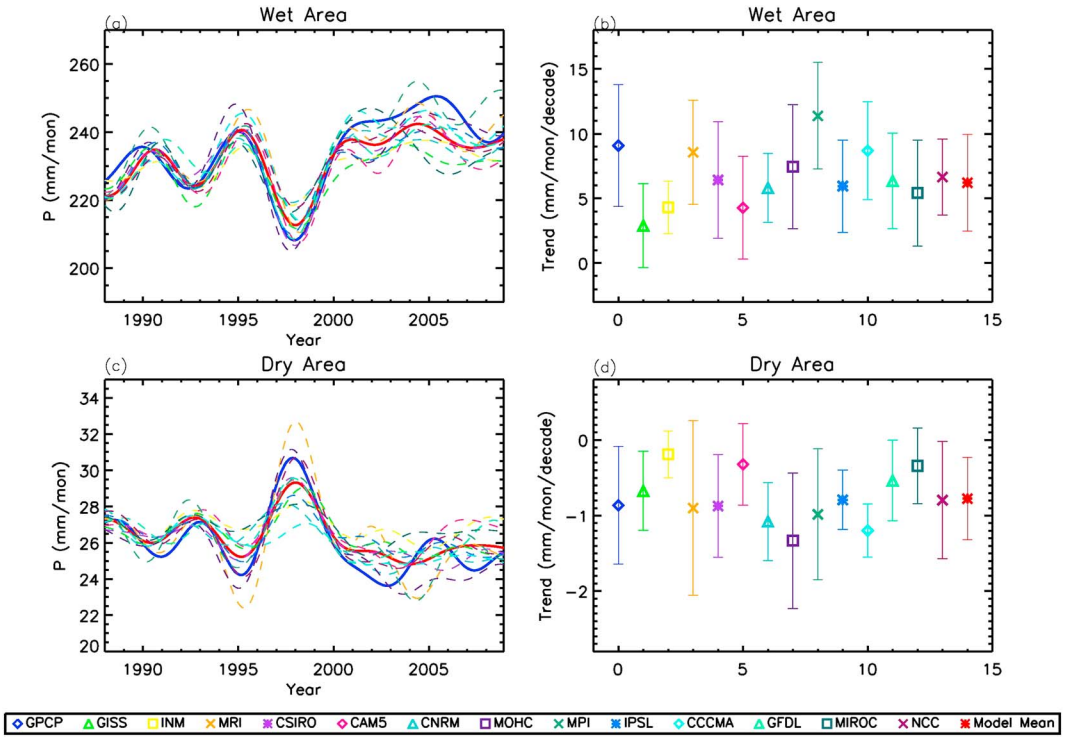


**Figure 2.** (a) Temporal variations of precipitation over wet areas ($P > 200$ mm/mon) between 60°N and 60°S. The color dashed lines represent results from 13 CMIP5 models. The red solid line represents the averaged precipitation from all model simulations. The blue solid line represents result from GPCP. (b) Trends and uncertainties for precipitation over wet areas from CMIP5 models and GPCP. (c and d) The same as Figures 2a and 2b except for dry areas ($P < 50$ mm/mon).

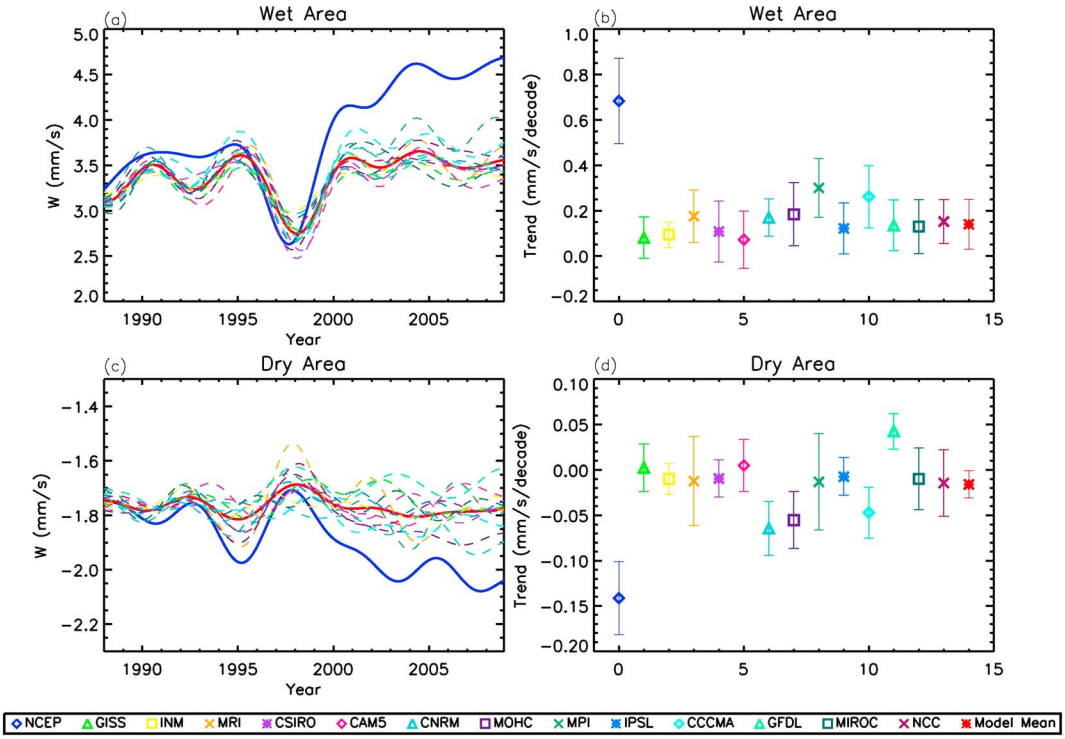


**Figure 3.** (a) Temporal variations of 500 hPa vertical velocity over wet areas ($P > 200$ mm/mon) between 60°N and 60°S. The color dashed lines represent results from 13 CMIP5 models. The red solid line represents the averaged vertical velocity from all model simulations. The blue solid line represents result from NCEP2 Reanalysis. (b) Trends and uncertainties for 500 hPa vertical velocity over wet areas from CMIP5 models and NCEP2. (c and d) The same as Figures 3a and 3b except for dry areas ($P < 50$ mm/mon).

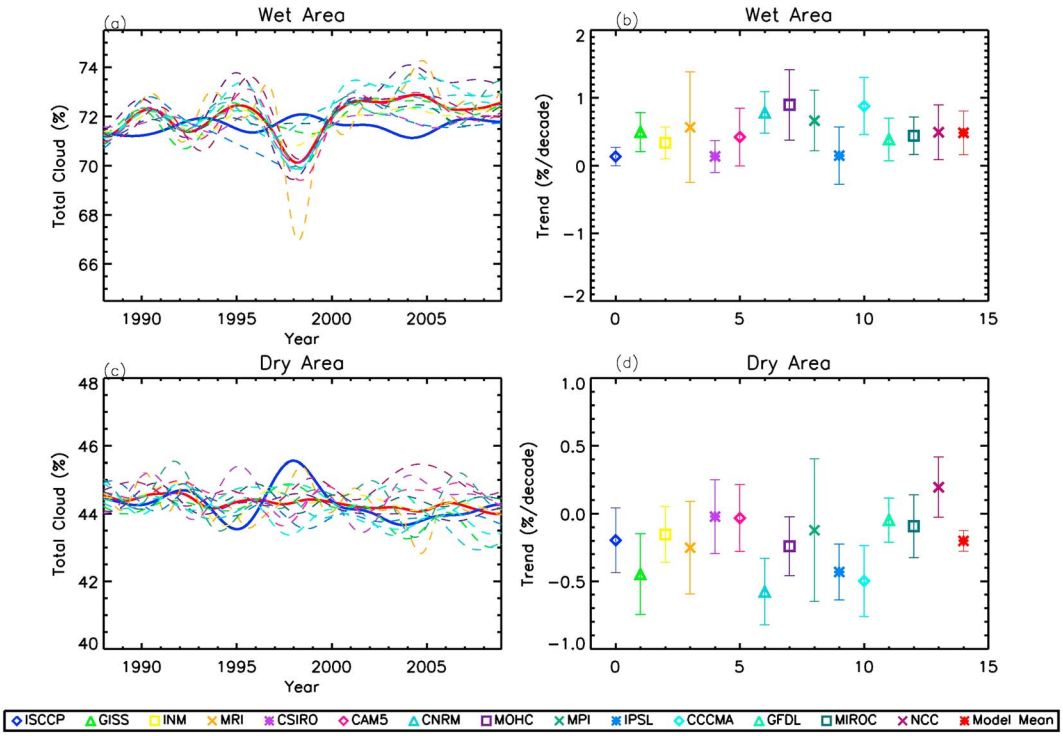


**Figure 4.** (a) Temporal variations of total cloud fraction over wet areas ($P > 200$ mm/mon) between 60°N and 60°S. The color dashed lines represent results from 13 CMIP5 models. The red solid line represents the averaged total cloud fraction from all model simulations. The blue solid line represents result from ISCCP total cloud coverage. (b) Trends and uncertainties of total cloud fraction over wet areas from CMIP5 models and ISCCP. (c and d) The same as Figures 4a and 4b except for dry areas ($P < 50$ mm/mon).

receive less with a trend of −0.86 ± 0.77 mm/mon/decade. The least squares fitting is used to estimate the linear trends and uncertainties [*Bevington and Robinson*, 2003; *Li et al*., 2011]. The standard error of the linear trend is estimated by $\mathrm{SE}(b) = (\sigma/\sqrt{N_1})/\sqrt{(1/N_2)\sum x_1^2}$, where $\sigma$ is the standard deviation of the data, $N_1$ is the degrees of freedom of the data, $N_2$ is the length of the data set, and $x_i$ is the time series [*Bevington and Robinson*, 2003; *Li et al*., 2011]. Precipitations from CMIP5 models calculated over wet and dry areas are plotted as color dashed lines in Figures 2a and 2c. All models are able to capture similar temporal variations of precipitation as that from the GPCP precipitation over wet areas and dry areas. As shown in Figure 2b, all models capture positive trends of precipitation over wet areas with a range from 2.9 mm/mon/decade to 11.4 mm/mon/decade. The trend of multimodel mean precipitation over wet areas is 6.22 ± 3.75 mm/mon/decade, which is smaller than the GPCP precipiation trend (9.09 ± 4.69 mm/mon/decade). All models also capture the negative trends of precipitation over dry areas with a range from −1.33 mm/mon/decade to −0.19 mm/mon/decade as shown in Figure 2d. The trend of multimodel mean precipitation over dry areas is −0.77 ± 0.54 mm/mon/decade, which is weaker than the GPCP precipitation trend (−0.86 ± 0.77 mm/mon/decade). This suggests that the models are able to capture the precipitation variations with consistent sign but variable magnitudes.

To explain the trends of precipitation, we examine the 500 hPa vertical velocity from NCEP2 and CMIP5 models over wet and dry areas. Results are shown in Figure 3. Corresponding trends in NCEP2 500 hPa vertical velocity for the wet areas are 0.68 ± 0.18 mm/s/decade and −0.14 ± 0.04 mm/s/decade for the dry areas. The positive trend of vertical velocity over wet areas suggests that the vertical velocity is increasing over wet areas and can lead to increased precipitation. As shown in Figure 3c, NCEP2 500 hPa vertical velocity is negative over dry areas, which suggest that sinking air dominates over dry areas. Negative trend of NCEP2 vertical velocity means that the sinking air is strengthening over dry areas, which will lead to the decreased precipitation over dry areas as shown in Figure 2c. Trends of the 500 hPa vertical velocity from CMIP5 models are positive for all models over the wet area. The trend of multimodel mean vertical velocity over wet areas is 0.14 ± 0.11 mm/s/decade, which is weaker than that from NCEP2. Trends of 500 hPa vertical

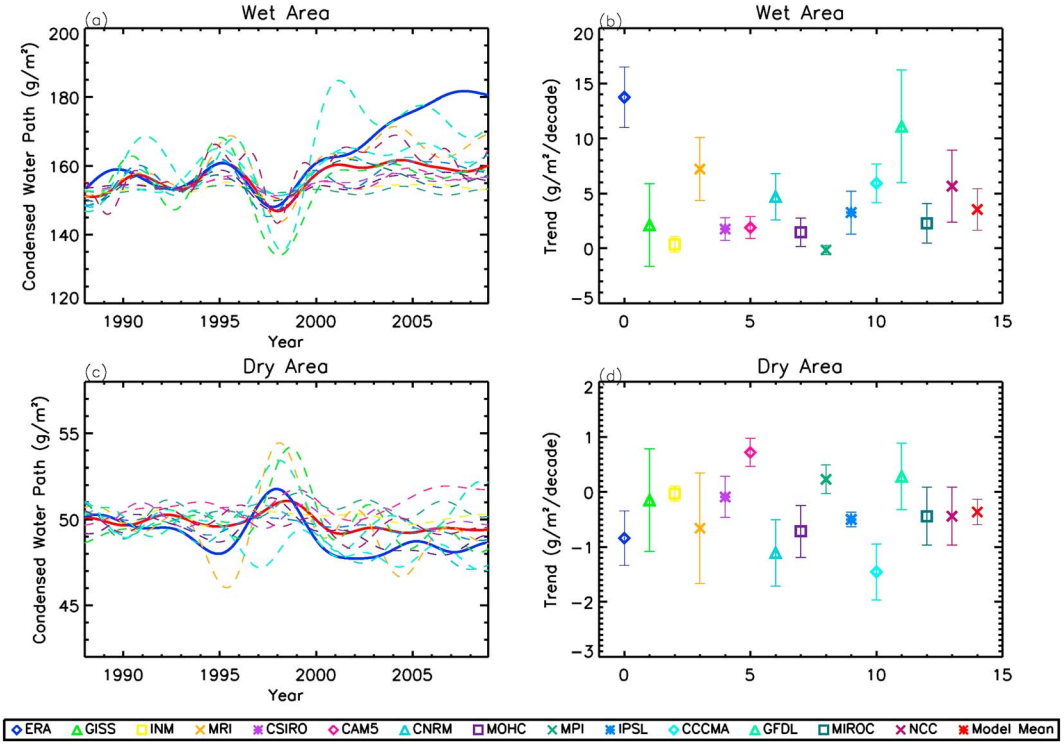


**Figure 5.** (a) Temporal variations of condensed water path over wet areas ($P > 200$ mm/mon) between 60°N and 60°S. The color dashed lines represent results from 13 CMIP5 models. The red solid line represents the averaged condensed water path from all model simulations. The blue solid line represents result from ECMWF. (b) Trends and uncertainties of condensed water path over wet areas from CMIP5 models and ECMWF. (c and d) The same as Figures 5c and 5b except for dry areas ($P < 50$ mm/mon).

velocities are negative for most models over the dry areas, as demonstrated in Figure 3d. The trend of multimodel mean vertical velocity over dry areas is −0.016 ± 0.015 mm/s/decade, which is also weaker than that from NCEP2 vertical velocity over the dry areas.

Cloud physics also plays important roles in precipitation, so we also explore cloud variations over wet areas and dry areas. Here the total cloud fraction, low cloud fraction, middle cloud fraction, high cloud fraction, condensed water path, and ice water path are investigated to see how the models are performing in simulating variations of clouds over the wet and dry regions. Figure 4a demonstrates the temporal variations of total cloud fraction from the ISCCP and CMIP5 models from 1988 to 2008. Trends for total cloud fraction over wet areas are shown in Figure 4b. ISCCP total cloud fraction demonstrates weak positive trend of 0.14 ± 0.1%/decade over wet areas. All models have an increasing tendency of total cloud fraction over the wet areas with a range from 0.14%/decade to 0.90%/decade. The trend of multimodel mean total cloud fraction over wet areas is 0.49 ± 0.32%/decade. The positive trends in clouds are related to the enhanced vertical velocity, which further lead to increasing precipitation over wet areas. When *Norris et al*. [2016] correct the raw ISCCP data, they remove global mean cloud variability from the data set. Since it is hard to separate trend from natural variability, we need be careful when we compare the model total cloud fraction results with the ISCCP. Figure 4c shows the total cloud fraction in dry areas. ISCCP total cloud fraction exhibits a weak negative trend of −0.2 ± 0.21%/decade over dry areas. The trend of multimodel mean total cloud fraction over dry areas is −0.20 ± 0.07%/decade. Most of the models show decreasing tendency of total cloud fraction in dry areas. Only the NCC model suggests an increasing total cloud fraction over dry areas. A possible explanation of total cloud fraction signals showing greater intermodel variability over the dry areas is the fact that there are very few clouds present in dry areas. In addition to the total cloud fraction, we also explore the variations of low cloud fraction, middle cloud fraction, and high cloud fraction from different models. Results are shown in Figures S1–S3 in the supporting information. As shown in Figures S1–S3, most models capture the positive trends of clouds at low, middle, and high altitudes over wet areas and negative trends of low, middle, and high clouds over dry areas.

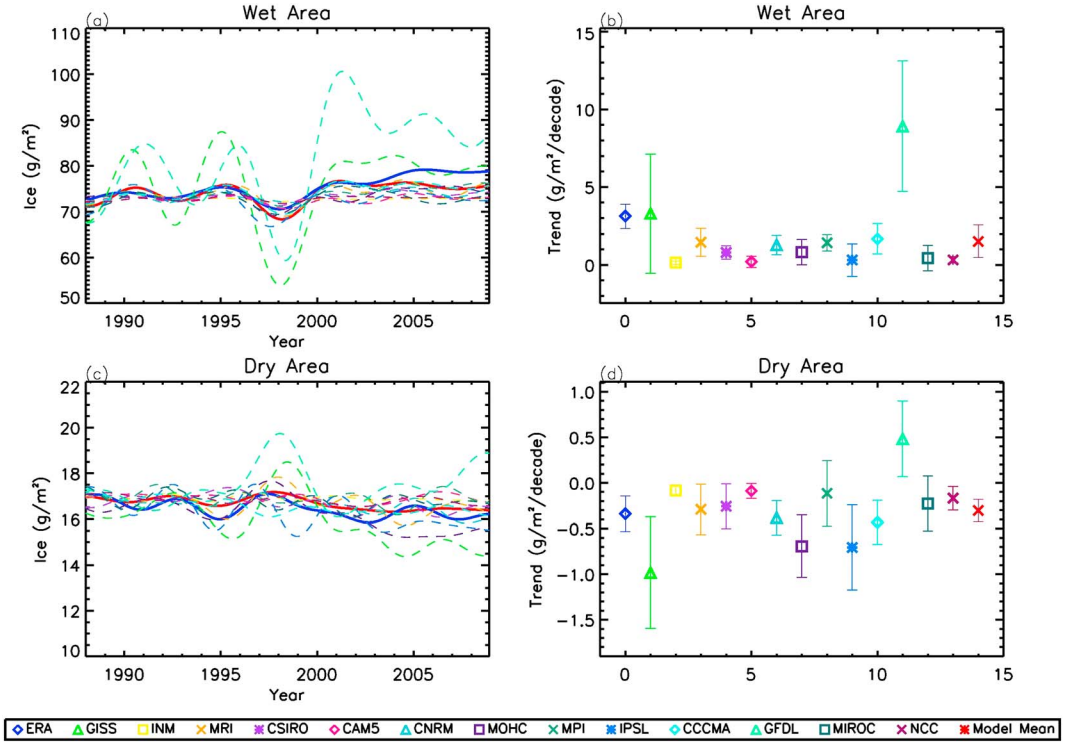


**Figure 6.** (a) Temporal variations of ice water path over wet areas ($P > 200$ mm/mon) between 60°N and 60°S. The color dashed lines represent results from 13 CMIP5 models. The red solid line represents the averaged ice water path from all model simulations. The blue solid line represents result from ECMWF. (b) Trends and uncertainties of ice water path over wet areas from CMIP5 models and ECMWF. (c and d) The same as Figures 6a and 6b except for dry areas ($P < 50$ mm/mon).

In addition to the cloud fractions, ice and liquid contents in the clouds are also explored in the wet and dry areas. Figure 5 shows the temporal variations of condensed water path at wet and dry areas over the past two decades. Condensed water path is defined as the mass of condensed liquid and ice water in the column, divided by the area of the column. Trends of ECMWF condensed water path for the wet areas are $13.7 \pm 2.7$ g/m$^2$/decade and $-0.8 \pm 0.4$ g/m$^2$/decade for the dry areas. The positive trend of condensed water path over wet areas suggests that the condensed water path is increasing over wet areas, which will lead to increased precipitation over wet areas. As shown in Figure 5c, the trend of ECMWF condensed water path is negative over dry areas, which is related to the decreased precipitation over dry areas. All of the models demonstrate consistent increasing tendency of condensed water path over the wet regions, although the trends of model condensed water path are smaller than that of ECMWF condensed water path. The trend of multimodel mean condensed water path over wet areas is $3.5 \pm 1.8$ g/m$^2$/decade, which is smaller than the trend of ECMWF condensed water path. Not all models simulated decreasing trends of liquid and ice contents in the dry regions. The trend of multimodel mean condensed water path over dry areas is $-0.4 \pm 0.2$ g/m$^2$/decade, which is weaker than that of ECMWF condensed water path. CAM5 and GFDL suggest increasing trends of liquid and ice content in the dry regions with some other models having no significant trends over the dry areas.

The ice crystal growth is important in developing precipitation [*Harper*, 2007], so the ice water paths are also investigated. Ice water path is defined as the mass of ice water in the column divided by the area of a column. Figure 6a shows the ice water path averaged over wet areas from 1988 to 2008. As shown in Figure 6b, ECMWF data and all models show a small increase in ice content in the cloud over wet areas. The trend of multimodel mean ice water path over wet areas is $1.5 \pm 1.0$ g/m$^2$/decade, which is smaller than the trend of ECMWF ice water path ($3.1 \pm 0.7$ g/m$^2$/decade) for wet areas. GISS and GFDL models indicate much larger trends of ice contents than other CMIP5 models over wet areas. There are possibilities of increasing the amount of convective clouds, which tend to contain higher ice contents, as they can grow higher up in the atmosphere. The rest of the models have very weak positive trends of ice contents over wet areas. Figure 6d shows the trends of ice contents over dry areas from ECMWF and all models. The trend of

ECMWF ice water path is $-0.3 \pm 0.1$ g/m$^2$/decade for the dry areas. Most models suggest negative trends of ice water contents over dry areas, except the GFDL model. The trend of the multimodel mean ice water path over dry areas is $-0.3 \pm 0.1$ g/m$^2$/decade, which is comparable to that from ECMWF ice water path. Since there are very few clouds present in the dry areas to begin with, the ice water path are very hard to simulate and show large intermodel variability.

Our analyses of vertical velocity, cloud fractions, condensed water path, and ice water path from CMIP5 model simulations provide a clearer picture of the dynamics and physics behind the temporal variation of precipitation over wet and dry areas. Over the wet areas, the positive trends of vertical velocity suggest the strengthening of the rising motion, which can further improve the cloud formation. With the increasing cloud fraction, the ice and liquid water contents in clouds increase. The increasing liquid/ice water contents quicken some important microphysical processes in developing precipitation (e.g., collision, coalescence, and aggregation) [*Salby*, 2012]. On the other hand, the weakening vertical motion in the dry areas does not favor the cloud formation, so that the related precipitation-developing mechanisms are suppressed. Therefore, the precipitation decreases over the dry areas.

## 5. Conclusion

Temporal variations of precipitation, vertical velocity, total cloud fraction, low cloud fraction, middle cloud fraction, high cloud fraction, condensed water path, and ice water path are explored over wet and dry areas from 1988 to 2008. CMIP5 models capture similar precipitation trends over wet and dry areas as those from GPCP precipitation estimates. To investigate possible reasons for temporal variations of precipitation, we examine 500 hPa vertical velocity over wet and dry areas. Most CMIP5 models capture positive trends of vertical velocity over wet areas and negative trends of vertical velocities over dry areas, although the magnitudes are weaker than that from NCEP2 vertical velocity. Total cloud fractions have increased over the wet areas for all CMIP5 models and ISCCP data. The increasing vertical velocity over the wet areas leads to more cloud coverage over wet areas, which can produce more precipitation over wet areas. Although it is very hard to simulate cloud patterns in the dry areas due to very few clouds present over the region, most of the models simulate slight decreasing trend of total clouds over the dry areas.

Most of the models also perform well in capturing variations of condensed water path and ice water path, although the magnitudes of trends of condensed water path and ice water path from CMIP5 are smaller than those from ECMWF. Liquid and ice contents demonstrate increasing trend over the wet areas and decreasing trends over the dry areas. GFDL is an exception in showing increasing ice content over both wet and dry regions and larger increasing trend than any other models over the wet areas. The overall model performances are reasonable in capturing the cloud variations over wet and dry regions. The results obtained from this study can help better characterize the variability of precipitation, vertical velocity, clouds, liquid, and ice water contents over wet areas and dry areas, which are important for a better simulation of the precipitation and to understand the long-term variations of these variables.

The analyses of numerical simulations from the CMIP5 models reveal qualitatively consistent trends in some of these variables (e.g., vertical velocity, clouds, liquid, and ice water contents) related to precipitation. These consistent trends provide a better picture of the dynamics and physics related to the temporal variations of precipitation, in which the vertical motions affect the cloud formation and the liquid/ice contents, which further influence the developing mechanisms of precipitation.

**Acknowledgments**
We thank an anonymous reviewer and the Editor for their time and helpful comments. The authors (Jiang and Kao) at the University of Houston and coauthor (Yung) at the California Institute of Technology were supported by NASA grants NNX13AC04G and NNX13AK34G. The coauthor (Su) at the Jet Propulsion Laboratory, California Institute of Technology, under contract with NASA, acknowledges the funding support from the NASA NEWS project. The coauthor (Li) at the University of Houston was supported by the NASA PDART program. GPCP V2.2 data are provided by the center of Earth System Research Laboratory at http://www.esrl.noaa.gov/psd/data/gridded/data.gpcp.html. NCEP2 data are available at http://www.esrl.noaa.gov/psd/data/gridded/data.ncep.reanalysis2.html.

## References

Adler, R. F., et al. (2003), The version 2 Global Precipitation Climatology Project (GPCP) monthly precipitation analysis (1979–present), *J. Hydrometeorol.*, *4*, 1147–1167.

Adler, R. F., G. J. Gu, J. J. Wang, G. J. Huffman, S. Curtis, and D. Bolvin (2008), Relationships between global precipitation and surface temperature on interannual and longer timescales (1979–2006), *J. Geophys. Res.*, *113*, D22104, doi:10.1029/2008JD010536.

Allan, R. P., and B. J. Soden (2007), Large discrepancy between observed and simulated precipitation trends in the ascending and descending branches of the tropical circulation, *Geophys. Res. Lett.*, *34*, L18705, doi:10.1029/2007GL031460.

Allan, R. P., and B. J. Soden (2008), Atmospheric warming and the amplification of precipitation extremes, *Science*, *321*, 1481–1484.

Allan, R. P., B. J. Soden, V. O. John, W. Ingram, and P. Good (2010), Current changes in tropical precipitation, *Environ. Res. Lett.*, *5*, 025205, doi:10.1088/1748-9326/5/2/025205.

Allen, M. R., and W. J. Ingram (2002), Constraints on future changes in climate and the hydrological cycle, *Nature*, *419*, 224–232.

Bevington, P. R., and D. K. Robinson (2003), *Data Reduction and Error Analysis for the Physical Sciences*, 3rd ed., McGraw-Hill, New York.

Bony, S., G. Bellon, D. Klocke, S. Sherwood, S. Fermepin, and S. Denvil (2013), Robust direct effect of carbon dioxide on tropical circulation and regional precipitation, *Nat. Geosci.*, *6*, 447–451.
Chou, C., and J. D. Neelin (2004), Mechanisms of global warming impacts on regional tropical precipitation, *J. Clim.*, *17*, 2688–2701.
Chou, C., J. D. Neelin, C. A. Chen, and J. Y. Tu (2009), Evaluating the "rich-get-richer" mechanism in tropical precipitation change under global warming, *J. Clim.*, *22*, 1982–2005.
Chou, C., J. C. H. Chiang, C. Lan, C. Chung, Y. Liao, and C. Lee (2013), Increase in the range between wet and dry season precipitation, *Nat. Geosci.*, *6*, 263–267.
Delanoe, J., R. J. Hogan, R. M. Forbes, A. Bodas-Salcedo, and T. H. M. Stein (2011), Evaluation of ice cloud representation in the ECMWF and UK Met Office models using Cloudsat and CALLPSO data, *Q. J. R. Meteorol. Soc.*, *137*, 2064–2078.
Dolinar, E. K., X. Dong, B. Xi, J. H. Jiang, and H. Su (2014), Evaluation of CMIP5 simulated clouds and TOA radiation budgets using NASA satellite observations, *Clim. Dyn.*, *44*, 2229, doi:10.1007/s00382-014-2158-9.
Donat, M. G., A. L. Lowry, L. V. Alexander, P. A. O'Gorman, and N. Maher (2016), More extreme precipitation in the world's dry and wet regions, *Nat. Clim. Change*, *6*, 508–513.
Durack, P. J., S. E. Wijffels, and R. J. Matear (2012), Ocean salinities reveal strong global water cycle intensification during 1950 to 2000, *Science*, *27*, 455–458.
Greve, P., B. Orlowsky, B. Mueller, J. Sheffield, M. Reichstein, and S. L. Seneviratne (2014), Global assessment of trends in wetting and drying over land, *Nat. Geosci.*, *7*, 716–721.
Gu, G. J., and R. F. Adler (2013), Interdecadal variability/long-term changes in global precipitation patterns during the past three decades; global warming and/or pacific decadal variability, *Clim. Dyn.*, *40*, 3009–3022.
Gu, G. J., R. F. Adler, G. J. Huffman, and S. Curtis (2007), Tropical rainfall variability on interannual-to-interdecadal and longer time scales derived from the GPCP monthly product, *J. Clim.*, *20*, 4033–4046.
Harper, K. (2007), *Weather and Climate: Decade by Decade, Twentieth-Century Science*, pp. 74–75, Infobase Pub., New York.
Hegerl, G. C., et al. (2015), Challenges in quantifying changes in the global water cycle, *Bull. Am. Meteorol. Soc.*, *96*, 1097–1115.
Held, I. M., and B. J. Soden (2006), Robust responses of the hydrological cycle to global warming, *J. Clim.*, *19*, 5686–5699.
Huffman, G. J., R. F. Adler, P. Arkin, A. Chang, R. Ferraro, A. Gruber, J. Janowiak, A. McNab, B. Rudolf, and U. Schneider (1997), The Global Precipitation Climatology Project (GPCP) combined precipitation data set, *Bull. Am. Meteorol. Soc.*, *78*, 5–20.
Huffman, G. J., D. T. Bolvin, and R. F. Adler (2012), *GPCP Version 2.2 Combined Precipitation Data Set*, NCDC, Asheville, N. C.
Jiang, J. H., et al. (2012), Evaluation of cloud and water vapor simulations in CMIP5 climate models using NASA A-Train satellite observations, *J. Geophys. Res.*, *117*, D14105, doi:10.1029/2011JD017237.
Jiang, J. H., et al. (2015), Evaluating the diurnal cycle of upper tropospheric ice clouds in climate models using SMILES observations, *J. Atmos. Sci.*, *72*, 1022–1044, doi:10.1175/JAS-D-14-0124.1.
Jiang, X., C. Camp, R. Shia, D. Noone, C. Walker, and Y. L. Yung (2004), Quasi-biennial oscillation and quasi-biennial oscillation-annual beat in the tropical total column ozone: A two-dimensional model simulation, *J. Geophys. Res.*, *109*, D16305, doi:10.1029/2003JD004377.
Kistler, R., et al. (2001), The NCEP-NCAR 50-year reanalysis: Monthly means CD-ROM and documentation, *Bull. Am. Meteorol. Soc.*, *82*, 247–267.
Li, L., X. Jiang, M. T. Chahine, E. T. Olsen, E. J. Fetzer, L. Chen, and Y. L. Yung (2011), The recycling rate of atmospheric moisture over the past two decades (1988–2009), *Environ. Res. Lett.*, *6*, 034017, doi:10.1088/1748-9326/6/3/034017.
Liu, C., and R. Allan (2013), Observed and simulated precipitation responses in wet and dry regions 1850–2100, *Environ. Res. Lett.*, *8*, 034002, doi:10.1088/1748-9326/8/3/034002.
Liu, C., R. Allan, and G. J. Huffman (2012), Co-variation of temperature and precipitation in CMIP5 models and satellite observations, *Geophys. Res. Lett.*, *39*, L13803, doi:10.1029/2012GL052093.
Liu, S. C., C. B. Fu, C. J. Shiu, J. P. Chen, and F. T. Wu (2009), Temperature dependence of global precipitation extremes, *Geophys. Res. Lett.*, *36*, L17702, doi:10.1029/2009GL040218.
Long, S., S. P. Xie, and W. Liu (2016), Uncertainty in tropical rainfall projections: atmospheric circulation effect and the ocean coupling, *J. Clim.*, *29*, 2671–2687.
Marvel, K., and C. Bonfils (2013), Identifying external influences on global precipitation, *Proc. Nati. Acad. Sci. U.S.A.*, *110*, 19,301–19,306.
Norris, J. R., R. J. Allen, A. T. Evan, M. D. Zelinka, C. W. O'Dell, and S. A. Klein (2016), Evidence for climate change in the satellite cloud record, *Nature*, *536*, 72–75, doi:10.1038/nature18273.
Polson, D., G. C. Hegerl, R. P. Allan, and B. Balan Sarojini (2013), Have greenhouse gases intensified the contrast between wet and dry regions? *Geophys. Res. Lett.*, *40*, 4783–4787, doi:10.1002/grl.50923.
Salby, M. L. (2012), *Physics of the Atmosphere and Climate*, 718 pp., Cambridge Univ. Press, New York.
Sarojini, B. B., P. A. Stott, and E. Black (2016), Detection and attribution of human influence on regional precipitation, *Nat. Clim. Change*, *6*, 669–675, doi:10.1038/NCLIMATE2976.
Shindell, D. T., G. Faluvegi, R. L. Miller, G. A. Schmidt, J. E. Hansen, and S. Sun (2006), Solar and anthropogenic forcing of tropical hydrology, *Geophys. Res. Lett.*, *33*, L24706, doi:10.1029/2006GL027468.
Stanfield, R. E., J. H. Jiang, X. Dong, B. Xi, H. Su, L. Donner, L. Rotstayn, T. Wu, J. Cole, and E. Shindo (2016), A quantitative assessment of precipitation associated with the ITCZ in the CMIP5 GCM simulations climate dynamics, *Clim. Dyn.*, *47*, 1863–1880, doi:10.1007/s00382-015-2937-y.
Stephens, G. L., and T. D. Ellis (2008), Controls of global-mean precipitation increases in global warming GCM experiments, *J. Clim.*, *21*, 6141–6155.
Su, H., et al. (2013), Diagnosis of regime-dependent cloud simulation errors in CMIP5 models using A-Train satellite observations, *J. Geophys. Res. Atmos.*, *118*, 2762–2780, doi:10.1029/2012JD018575.
Su, H., J. H. Jiang, C. X. Zhai, T. J. Shen, J. D. Neelin, G. L. Stephens, and Y. L. Yung (2014), Weakening and strengthening structures in the Hadley circulation change under global warming and implications for cloud response and climate sensitivity, *J. Geophys. Res. Atmos.*, *119*, 5787–5805, doi:10.1002/2014JD021642.
Su, H., et al. (2017), Tightening of tropical ascent and high clouds key to precipitation change in a warmer climate, *Nat. Commun.*, *8*, 15,771, doi:10.1038/ncomms15771.
Sun, F., M. L. Roderick, and G. D. Farquhar (2012), Changes in the variability of global land precipitation, *Geophys. Res. Lett.*, *39*, L19402, doi:10.1029/2012GL053369.
Taylor, K. E., R. J. Stouffer, and G. A. Meehl (2012), An overview of CMIP5 and the experiment design, *Bull. Am. Meteorol. Soc.*, *93*, 485–498.
Trammell, J. H., X. Jiang, L. Li, M. Liang, M. Li, J. Zhou, E. Fetzer, and Y. Yung (2015), Investigation of precipitation variations over wet and dry areas from observation and model, *Adv. Meteorol.*, *2015*, 1–9.

Trenberth, K. E., and D. J. Shea (2005), Relationships between precipitation and surface temperature, *Geophys. Res. Lett.*, *32*, L14703, doi:10.1029/2005GL022760.

Wang, Y., J. H. Jiang, and H. Su (2015), Atmospheric responses to the redistribution of anthropogenic aerosols, *J. Geophys. Res. Atmos.*, *120*, 9625–9641, doi:10.1002/2015JD023665.

Xie, S. P., et al. (2015), Towards predictive understanding of regional climate change, *Nat. Clim. Change*, *5*, 921–930.

Zhang, X., F. W. Zwiers, G. C. Hegerl, F. H. Lambert, N. P. Gillett, S. Solomon, P. A. Stott, and T. Nozawa (2007), Detection of human influence on twentieth-century precipitation trends, *Nature*, *448*, 461–465.

Zhai, C., J. H. Jiang, and H. Su (2015), Long term cloud change imprinted in seasonal cloud variation: More evidence of high climate sensitivity, *Geophys. Res. Lett.*, *42*, 9729–8737, doi:10.1002/2015GL065911.